Competitive Reactivity of W–C, W–N, and W–O Bonds at the Cp*W(NO) Fragment: Insertion Reactions of *tert*-Butyl Isocyanide, *p*-Tolyl Isocyanate, and Carbon Disulfide[1]

Peter Legzdins,* Steven J. Rettig, and Kevin J. Ross

Department of Chemistry, The University of British Columbia, Vancouver, British Columbia, Canada V6T 1Z1

Received November 9, 1993®

The three related complexes, Cp*W(NO)(CH_2CMe_3)($NHCMe_3$) (**1**), Cp*W(NO)($OCMe_3$)($NHCMe_3$) (**2**), and Cp*W(NO)($OCMe_3$)(CH_2CMe_3) (**3**), which differ only in the nature of the pair of groups α to the metal center, have been treated with *tert*-butyl isocyanide, *p*-tolyl isocyanate, and carbon disulfide in order to establish the relative tendencies of the W–C, W–N, and W–O linkages to undergo insertions of these reagents. The only site of insertion for *tert*-butyl isocyanide is the W–C bond, the W–N and W–O linkages being unreactive toward this substrate. In contrast, the preferential site of insertion for the two heterocumulenes, *p*-tolyl isocyanate, and carbon disulfide, was found to be W–N > W–O > W–C and W–N ≅ W–C > W–O, respectively. These observations can be rationalized in terms of two different mechanisms being operative, one involving initial adduct formation at the metal center and the other involving direct attack at the tungsten–element bond undergoing the insertion. The *tert*-butyl isocyanide reactions proceed predominantly via the former mechanism, the *p*-tolyl isocyanate reactions proceed predominantly via the latter mechanism, and the carbon disulfide reactions proceed via both mechanistic pathways simultaneously. Consistently, a kinetic investigation of the reaction between complex **2** and *p*-tolyl isocyanate reveals that the reaction is second-order overall and first-order in **2** in the presence of an excess of isocyanate, findings indicative of a simple bimolecular reaction between **2** and the isocyanate. The solid-state molecular structure of Cp*W(NO)(η^2-C{$NCMe_3$}CH_2CMe_3)($OCMe_3$) (**5**), formed by the reaction of **3** with *tert*-butyl isocyanide, has been established by a single-crystal X-ray diffraction analysis. Crystals of **5** are orthorhombic, space group *Pbca*, with a = 17.459(2) Å, b = 20.393(3) Å, c = 15.075(3) Å, and Z = 8; the structure was solved by conventional heavy-atom methods and was refined by full-matrix least-squares procedures to R_F = 0.032 and R_{wF} = 0.027 for 3856 reflections with $I \geq 3\sigma(I)$. Finally, the reactivity of **1**–**3** and the related chloro complexes, Cp*W(NO)($XCMe_3$)Cl (X = NH, CH_2 and O), with CO_2 has also been investigated and indicates that, in general, the W–N linkage is the preferential site of CO_2 insertion.

Introduction

Many homogeneous catalytic processes involve transition metal–carbon, –oxygen, and –nitrogen bonds.[2] Consequently, the study of the tendency of such bonds to undergo basic transformations such as insertions of small molecules is of fundamental importance. By far, most attention has been focused on the reactivity of metal–carbon bonds toward insertions of carbon monoxide, carbon dioxide, and alkenes and alkynes.[3] The same reactions with metal–nitrogen and metal–oxygen bonds have been less studied and are thus not as well understood. In general, the comparative reactivity of these bonds at the same metal centers remains to be established.

The studies of metal–carbon bonds include investigations of competitive carbonylation involving M–C and M–C′ linkages in complexes of the type $Cp_2M(R)(R')$.[4] These studies have established that, in general, insertion of CO occurs into the most sterically hindered M–C bond. Similar findings have also been reported recently for a series of asymmetric Cp*W(NO)(R)(R′) complexes.[5] In comparison, much less effort has been devoted to investigating the competitive reactivity of M–C vs M–O or M–N bonds. One such study involved the metallacyclic ruthenium complexes shown below, and it demonstrated that the preferential site of insertion of CO and CO_2 is the $M–C_{aryl}$ bond and not the $M–C_{alkyl}$, M–O, or M–N bonds.[6] The present study involves the comparative insertions of *tert*-butyl isocyanide, *p*-tolyl isocyanate, and carbon disulfide into the tungsten–carbon, –nitrogen, and –oxygen bonds of the related complexes Cp*W(NO)(CH_2CMe_3)($NHCMe_3$) (**1**), Cp*W(NO)($OCMe_3$)($NHCMe_3$) (**2**), and Cp*W(NO)(CH_2CMe_3)($OCMe_3$) (**3**) whose syntheses we have recently reported.[7] These complexes contain pairs of ligands of the type $XCMe_3$ (X = CH_2, NH, O) which,

* Abstract published in *Advance ACS Abstracts*, January 1, 1994.

(1) Presented in part at the 206th American Chemical Society National Meeting, Chicago, IL, Aug 1993; Abstract INOR 467.

(2) Parshall, G. W.; Ittel, S. D. *Homogeneous Catalysis: The Applications and Chemistry of Catalysis by Soluble Transition Metal Complexes*; Wiley-Interscience: New York, 1992.

(3) Collman, J. P.; Hegedus, L. S.; Norton, J. R.; Finke, R. G. *Principles and Applications of Organotransition Metal Chemistry*; University Science Books: Mill Valley, CA, 1987; Chapter 5.

(4) (a) Jeffery, J.; Lappert, M. F.; Luong-Thi, N. T.; Webb, M.; Atwood, J. L.; Hunter, W. E. *J. Chem. Soc., Dalton Trans.* **1981**, 1593. (b) Lappert, M. F.; Luong-Thi, N. T.; Milne C. *J. Organomet. Chem.* **1979**, *174*, C35.

(5) The bis(hydrocarbyl) systems, Cp*W(NO)(R)(R′), have been utilized to establish the relative aptitudes of the R and R′ ligands toward CO insertion, see: Debad, J. D.; Legzdins, P.; Einstein, F. W. B.; Batchelor, R. J. *Organometallics* **1993**, *12*, 2094.

(6) The reaction of the ruthenium arylamide complex with CO_2, however, does result in formal insertion into the Ru–N linkage, see: Hartwig, J. F.; Bergman, R. G.; Anderson, R. A. *J. Am. Chem. Soc.* **1991**, *113*, 6499.

(7) Legzdins, P.; Rettig, S. J.; Ross, K. J. *Organometallics* **1993**, *12*, 2103.

0276-7333/94/2313-0569$04.50/0

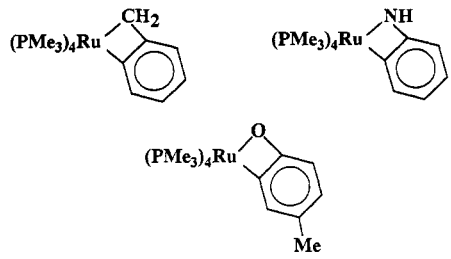

because of their similar steric demands, provide a unique opportunity to effect a comparative study of their electronic tendencies to undergo insertion at the same metal center.

Two heterocumulenes, *p*-tolyl isocyanate and CS_2, and *tert*-butyl isocyanide, a valence-isoelectronic analogue of CO, were chosen as representative reagents for studies in this regard with complexes **1–3**. Preliminary reactivity studies involving CO_2 have also been carried out.

Experimental Section

General procedures routinely employed in these laboratories have been described in detail previously.[8] Carbon disulfide (Aldrich) was distilled from P_2O_5 and *p*-tolyl isocyanate (Aldrich) was vacuum transferred from P_2O_5. Bone-dry CO_2 (99.999%, Matheson) and *tert*-butyl isocyanide (Aldrich) were used as received.

In most cases, reactions were performed in NMR tubes containing organometallic complex (50 mg, 0.10 mmol), excess organic reagent (0.2 mL), and C_6D_6 (0.7 mL). Upon completion of the reaction, the contents of the NMR tube were poured into a Schlenk tube in a glovebox. These solutions were taken to dryness in vacuo, and the viscous residues were triturated with pentane to obtain yellow to red powders. These powders were then dissolved in an appropriate solvent and crystallized. Due to the high solubility of most product complexes, the cited isolated yields of crystallized materials are not optimized. In some cases, the assignment of IR bands is not unambiguous due to the complexity of the spectra in the region 1650–1500 cm^{-1}.

Reaction of Cp*W(NO)(CH_2CMe_3)(NHCMe$_3$) (1) with Me_3CNC. An NMR tube containing **1**, Me_3CNC, and $CDCl_3$ (0.7 mL) was placed in an oil bath maintained at 70 °C for 1 d. After this period, the resonances attributable to the starting material were replaced by a new set of signals (>90% based on integration) in the ^1H NMR spectrum of the reaction mixture. Complex **4**, Cp*W(NO)(η^2-C{NCMe$_3$}CH_2CMe_3)Cl, was isolated as yellow needles (25 mg, 46% yield) from CH_2Cl_2/hexanes. The analytical and spectroscopic properties were identical with those previously reported for this complex.[9]

Reaction of Cp*W(NO)(OCMe$_3$)(NHCMe$_3$) (2) with Me_3CNC. An NMR tube containing **2**, Me_3CNC, and C_6D_6 was placed in an oil bath maintained at 100 °C for 5 d. As judged by ^1H NMR spectroscopy, no reaction had occurred. Longer reaction times and higher temperatures resulted in decomposition of the organometallic starting material.

Reaction of Cp*W(NO)(OCMe$_3$)(CH_2CMe_3) (3) with Me_3CNC. An NMR tube containing **3**, Me_3CNC, and C_6D_6 was maintained at ambient temperatures for 1 d whereupon it changed in color from red to yellow. After this period, the resonances attributable to the starting material were no longer evident in the ^1H NMR spectrum of the reaction mixture, but they had been replaced by a new set of signals (90% by integration). Complex **5**, Cp*W(NO)(η^2-C{NCMe$_3$}CH_2CMe_3)(OCMe$_3$), was isolated as yellow blocks (38 mg, 65% yield) from Et_2O.

Anal. Calcd for $C_{24}H_{44}N_2O_2W$: C, 50.00; H, 7.69; N, 4.86. Found: C, 50.30; H, 7.55; N, 4.96. IR (Nujol mull): ν_{CN} 1637 (m), ν_{NO} 1524 (s) cm^{-1}. ^1H NMR (C_6D_6): δ 3.08 (d ($^2J_{HH}$ = 14 Hz), 1H, $CH_ACH_BCMe_3$), 2.27 (d ($^2J_{HH}$ = 14 Hz), 1H, $CH_ACH_BCMe_3$), 1.76 (s, 15H, C_5Me_5), 1.53 (s, 9H, CMe_3), 1.27 (s, 9H, CMe_3), 1.19 (s, 9H, CMe_3). $^{13}C\{^1H\}$ NMR (C_6D_6): δ 225.40 (*C*N), 110.99 (C_5Me_5), 76.33 (O*C*Me$_3$), 58.24 (CN*C*Me$_3$), 45.85 (CH_2CMe_3), 32.53 (CH_2CMe_3), 34.24, 30.84, 30.26 (3 × C*Me*$_3$), 10.33 (C_5Me_5). Low-resolution mass spectrum (probe temperature 150 °C): *m/z* 576 [P^+].

Reaction of Cp*W(NO)(CH_2CMe_3)(NHCMe$_3$) (1) with *p*-Me-C_6H_4NCO. An NMR tube containing **1**, *p*-Me-C_6H_4NCO, and C_6D_6 was maintained at 20 °C, and the progress of the reaction was monitored by ^1H NMR spectroscopy for 5 d whereupon the isocyanate was consumed. The reaction mixture was taken to dryness in vacuo, the remaining residue was extracted with CH_2Cl_2 (2 × 5 mL), the extracts were filtered through Celite (2 × 2 cm) supported on a medium-porosity frit, and hexanes (10 mL) were added to the amber filtrate. Cooling of this solution to −30 °C led to the deposition of a white powder (60 mg, 30% approximate yield) which was identified by comparison to literature data[10] as (*p*-Me-$C_6H_4NCO)_x$. Varying the solvent and concentration of the reactants did not result in the production of the desired insertion product(s).

Reaction of Cp*W(NO)(OCMe$_3$)(NHCMe$_3$) (2) with *p*-Me-C_6H_4NCO. An NMR tube containing **2**, *p*-Me-C_6H_4NCO, and C_6D_6 was maintained at ambient temperatures, and the course of the reaction was monitored by ^1H NMR spectroscopy during 2 d, after which time the conversion was judged to be >98% complete. During this period, the resonances of the starting material were replaced by two sets of signals in the ratio of 8:1 which were assigned to the complexes **6**, Cp*W(NO)(η^2-N{*p*-Me-C_6H_4}C{O}NHCMe$_3$)(OCMe$_3$), and **6′**, Cp*W(NO)(η^2-N{*p*-Me-C_6H_4}C{O}OCMe$_3$)(NHCMe$_3$). Cooling of the reaction mixture in Et_2O at −30 °C afforded an orange powder (32 mg, 51% yield).

Anal. Calcd for $C_{26}H_{41}N_3O_3W$: C, 49.77; H, 6.58; N, 6.70. Found: C, 50.00; H, 6.56; N, 6.75. IR (Nujol mull): ν_{CO} 1556 (s), ν_{NO} 1530 (s), also 1505 (s), 1182 (m), 944 (s) cm^{-1}. ^1H NMR (C_6D_6): δ 7.22 (d ($^3J_{HH}$ = 8.4 Hz), 2H, *o*-C_6H_4), 7.03 (d ($^3J_{HH}$ = 8.4 Hz), 2H, *m*-C_6H_4), 4.6 (s, 1H, N*H*), 2.09 (s, 3H, *Me*), 1.91 (s, 15H, C_5Me_5), 1.52 (s, 9H, CMe_3), 1.12 (s, 9H, CMe_3). $^{13}C\{^1H\}$ NMR (CD_2Cl_2): δ 160.84 (*C*O), 145.28 (C_{ipso}), 135.19 (C_{para}), 129.70 (C_{meta}), 126.44 (C_{ortho}), 115.35 (C_5Me_5), 81.28 (O*C*Me$_3$), 50.99 (NH*C*Me$_3$), 33.33, 29.31 (2 × C*Me*$_3$), 21.03 (*Me*), 10.18 (C_5Me_5). Low-resolution mass spectrum (probe temperature 180 °C): *m/z* 627 [P^+].

Reaction of Cp*W(NO)(OCMe$_3$)(CH_2CMe_3) (3) with *p*-Me-C_6H_4NCO. An NMR tube containing **3**, *p*-Me-C_6H_4NCO, and C_6D_6 was maintained at ambient temperatures, and the progress of the reaction was monitored by ^1H NMR spectroscopy over 14 d, after which time the conversion was judged to be >98% complete. As the reaction progressed, the resonances due to the starting material were replaced by two sets of signals in the approximate ratio of 22:1 which were assigned to complexes **7**, Cp*W(NO)(η^2-N{*p*-Me-C_6H_4}C{O}OCMe$_3$)(CH_2CMe_3), and **7′**, Cp*W(NO)(η^2-N{*p*-Me-C_6H_4}C{O}CH_2CMe_3)(OCMe$_3$), respectively. Cooling of the reaction mixture in Et_2O at −30 °C afforded a yellow powder (38 mg, 60% yield).

Anal. Calcd for $C_{27}H_{42}N_2O_3W$: C, 51.76; H, 6.76; N, 4.47. Found: C, 51.95; H, 6.79; N, 4.61. IR (Nujol mull): 1538 (s(br)), also 1163 (m), 1056 (m) cm^{-1}. ^1H NMR (C_6D_6): δ 7.69 (d ($^3J_{HH}$ = 8.4 Hz), 2H, *o*-C_6H_4), 7.02 (d ($^3J_{HH}$ = 8.4 Hz), 2H, *m*-C_6H_4), 1.62 (s, 9H, CMe_3), 1.58 (s, 15H, C_5Me_5), 1.40 (d ($^2J_{HH}$ = 12.6 Hz), 1H, $CH_AH_BCMe_3$), 1.25 (s, 9H, CMe_3), 0.95 (d ($^2J_{HH}$ = 12.6 Hz), 1H, $CH_AH_BCMe_3$); discernible peaks for **7′**: δ 7.51 (d, *o*-C_6H_4), 6.97 (d, *m*-C_6H_4). $^{13}C\{^1H\}$ NMR (C_6D_6): δ 140.53 (C_{ipso}), 132.98 (C_{para}), 129.49 (C_{meta}), 125.0 (C_{ortho}), 110.13 (C_5Me_5), 83.02 (O*C*Me$_3$), 63.42 (CH_2CMe_3), 38.10 (CH_2CMe_3), 35.23, 28.58 (2 × C*Me*$_3$), 20.85 (*Me*), 9.30 (C_5Me_5), CO not observed. Low-resolution mass spectrum (probe temperature 180 °C): *m/z* 626 [P^+].

(8) Dryden, N. H.; Legzdins, P.; Rettig, S. J.; Veltheer, J. E. *Organometallics* **1992**, *11*, 2583.
(9) Debad, J. D.; Legzdins, P.; Rettig, S. J.; Veltheer, J. E. *Organometallics* **1993**, *12*, 2714.
(10) Legzdins, P.; Phillips, E. C.; Rettig, S. J.; Trotter, J.; Veltheer, J. E.; Yee, V. C. *Organometallics* **1992**, *11*, 3104.

Reaction of Cp*W(NO)(CH_2CMe_3)($NHCMe_3$) (1) with CS_2. An NMR tube containing complex 1, CS_2, and C_6D_6 was maintained at ambient temperatures, and the reaction was monitored by ^1H NMR spectroscopy for 6 d whereupon the conversion was judged to be >98% complete. During the course of the reaction the resonances of the starting material were replaced by two sets of signals in a ratio of 1:1 which were assigned to complexes 8, Cp*W(NO)(η^2-$S_2CCH_2CMe_3$)($NHCMe_3$), and 8′, Cp*W(NO)(η^2-$S_2CNHCMe_3$)(CH_2CMe_3). The dried reaction mixture was dissolved in Et_2O, and cooling of this solution to −30 °C led to the precipitation of a dark orange solid (42 mg, 74% yield).

Anal. Calcd for $C_{20}H_{36}N_2OS_2W$: C, 42.25; H, 6.38; N, 4.93. Found: C, 42.06; H, 6.29; N, 5.00. IR (Nujol mull): ν_{NO} 1532 (s), also 1506 (m), 1407 (m) cm^{-1}. ^1H NMR (C_6D_6): δ 6.85 (s, N*H*), 6.60 (s, N*H*), 1.73 (s, 2 × C_5Me_5), 1.47 (s, CMe_3), 1.45 (s, CMe_3), 1.17 (s, CMe_3), 1.13 (s, CMe_3), 1.05 (d ($^2J_{HH}$ = 13 Hz), $CH_AH_BCMe_3$), 0.99 (s, S_2CCH_2), 0.82 (d ($^2J_{HH}$ = 13 Hz), $CH_AH_BCMe_3$). $^{13}C\{^1H\}$ NMR (C_6D_6): δ 206.65, 206.42 (2 × S_2C), 108.45, 108.36 (2 × C_5Me_5), 56.28, 56.10 (2 × $NHCMe_3$), 52.58, 51.24 (2 × CH_2), 38.71 (CH_2CMe_3), 35.57, 35.45, 28.52, 28.40 (4 × CMe_3), 9.98, 9.86 (2 × C_5Me_5). Low-resolution mass spectrum (probe temperature 150 °C): *m/z* 566 [P^+], 492 [$P^+ - CS_2$].

Reaction of Cp*W(NO)($OCMe_3$)($NHCMe_3$) (2) with CS_2. An NMR tube containing 2, CS_2, and C_6D_6 was maintained at ambient temperatures for 5 d, and the progress of the reaction was monitored by ^1H NMR spectroscopy. As the conversion progressed, the resonances of the starting material were replaced by two sets of signals in the ratio of 8:1 which were assigned to complexes 9, Cp*W(NO)(η^2-$S_2CNHCMe_3$)($OCMe_3$), and 9′, Cp*W(NO)(η^2-S_2COCMe_3)($NHCMe_3$). The conversion was judged to be >98% complete after 5 d. The reaction mixture was dissolved in Et_2O/pentane (2:1), and cooling of this solution to −30 °C led to the isolation of an orange powder (30 mg, 52% yield).

Anal. Calcd for $C_{19}H_{34}N_2O_2S_2W$: C, 40.00; H, 6.01; N, 4.91. Found: C, 40.34; H, 6.05; N, 4.85. IR (Nujol mull): ν_{NO} 1557 (s), also 1526 (s), 1508 (s), 1406 (m), ν_{CS_2} 1178 (s) and 1022 (s) cm^{-1}. ^1H NMR (C_6D_6): δ 7.00 (s, 1H, N*H*), 1.84 (s, 15H, C_5Me_5), 1.50 (s, 9H, CMe_3), 1.16 (s, 9H, CMe_3). $^{13}C\{^1H\}$ NMR (C_6D_6): δ 203 (br, S_2C), 112.83 (C_5Me_5), 78.32 ($OCMe_3$), 56.31 ($NHCMe_3$), 34.28, 28.34, (2 × CMe_3), 10.14 (C_5Me_5); major peaks of 9′: 34.02, 28.07, (2 × CMe_3), 10.00 (C_5Me_5). Low-resolution mass spectrum (probe temperature 180 °C): *m/z* 570 [P^+], 540 [P^+ − NO].

Reaction of Cp*W(NO)($OCMe_3$)(CH_2CMe_3) (3) with CS_2. An NMR tube containing 3, CS_2, and C_6D_6 was placed in an oil bath maintained at 100 °C, and there was no reaction as determined by ^1H NMR spectroscopic monitoring over 7 d. Higher temperature simply caused decomposition to many (>5) products as judged by the number of peaks attributable to Cp* resonances.

Reaction of Complex 1 with CO_2. To an NMR tube was added 1 (50 mg, 0.10 mmol) and C_6D_6 (0.7 mL), and the tube was charged with CO_2 (ca. 15 psig). After 1 d the resonances attributable to the starting material had disappeared and had been replaced by a new set of signals (>99% conversion) that were indicative of the formation of Cp*W(NO)(η^2-$O_2CNHCMe_3$)(CH_2CMe_3) (10). The final reaction mixture was taken to dryness in vacuo, and the residue was recrystallized from Et_2O/pentane (1:1) at −30 °C to obtain orange crystals of complex 10 (34 mg, 63% yield).

Anal. Calcd for $C_{20}H_{36}N_2O_3W$: C, 44.78; H, 6.76; N, 5.22. Found: C, 44.93; H, 6.89; N, 5.03. IR (Nujol mull): ν_{CO_2} 1589 (s) and 1538 (s), ν_{NO} 1519 (s), also 1239 (m), 1215 (m) cm^{-1}. ^1H NMR (C_6D_6): δ 4.7 (s, 1H, N*H*), 1.68 (s, 15H, C_5Me_5), 1.62 (s, 9H, CMe_3), 1.24 (d ($^2J_{HH}$ = 13 Hz), 1H, $CH_AH_BCMe_3$), 1.04 (s, 9H, CMe_3), 0.97 (d ($^2J_{HH}$ = 13 Hz), 1H, $CH_AH_BCMe_3$). $^{13}C\{^1H\}$ NMR ($CDCl_3$): δ 165.98 (*OCO*), 111.09 (C_5Me_5), 65.60 (CH_2CMe_3), 50.20 ($NHCMe_3$), 37.92 (CH_2CMe_3), 34.92, 29.08 (2 × CMe_3), 9.29 (C_5Me_5). Low-resolution mass spectrum (probe temperature 150 °C): *m/z* 536 [P^+].

Treatment of Complexes 2 and 3 with CO_2. A benzene solution of complex 2 (50 mg) under 15 psig CO_2 was stirred in a glass bomb at room temperature for 1 d, during which time the solution darkened in color from light yellow to dark amber. The final solution was taken to dryness in vacuo, the residue was triturated to a dark orange powder with Et_2O, and the powder was redissolved in CH_2Cl_2 (20 mL). An orange powder precipitated upon cooling of the CH_2Cl_2 solution to −30 °C. This powder had IR (Nujol mull: 1647 (s), 1606 (s) and 1587 (s) cm^{-1}) and mass spectral (538 [P^+]) features indicative of the existence of the CO_2-inserted product, Cp*W(NO)(η^2-$O_2CNHCMe_3$)($OCMe_3$) (11). However, this product was impure as determined by ^1H NMR spectroscopy and has not yet been isolated in an analytically pure state. The reaction between 2 and CO_2 in C_6D_6 was also monitored by ^1H NMR spectroscopy which indicated that three major products were formed. Thermolysis of this reaction mixture at 80 °C overnight and subsequent cooling to room temperature led to the deposition of white crystals of $(Me_3CNH)_2CO$ which were isolated by cannulating away the mother liquor. The organic compound was identified by its spectroscopic properties: ^1H NMR ($CDCl_3$): δ 4.0 (s(br), 1H, N*H*), 1.29 (s, 9H, CMe_3). IR (Nujol mull): ν_{CO} 1640 cm^{-1}. Low-resolution mass spectrum (probe temperature 150 °C): 172 [P^+].

A solution of complex 3 in benzene was prepared and treated with CO_2 as described in the preceding paragraph. The solution was stirred for 1 d at ambient temperatures, and the final solution was taken to dryness in vacuo. IR and NMR spectra of the residue confirmed that no reaction had occurred.

Treatment of Cp*W(NO)(CH_2CMe_3)Cl and Cp*W(NO)($OCMe_3$)Cl with CO_2. Benzene solutions of these complexes (50 mg) were made up in a glass bomb equipped with a Kontes stopcock, and the vessels were then pressurized to approximately 15 psig with CO_2. The resulting solutions were stirred at room temperature for 1 d with no color changes occurring. The solutions were taken to dryness in vacuo, and IR and NMR spectra of the residues confirmed that no reactions had occurred.

Reaction of Cp*W(NO)($NHCMe_3$)Cl with CO_2. A solution of Cp*W(NO)($NHCMe_3$)Cl (450 mg, 1.0 mmol) in benzene (10 mL) was prepared in a glass bomb equipped with a Kontes stopcock, and the vessel was pressurized to approximately 15 psig with CO_2. Over a period of 1 d at ambient temperatures, the orange color of the solution lightened. The final solution was taken to dryness in vacuo, the residue was triturated with Et_2O, and the resulting solid was extracted with CH_2Cl_2 (20 mL). The extract was filtered through Celite (2 × 3 cm) supported on a medium-porosity frit. The light orange filtrate was reduced in volume in vacuo and was placed in a freezer at −30 °C to induce the deposition of Cp*W(NO)(η^2-$O_2CNHCMe_3$)Cl (12) as an orange powder (350 mg, 71% yield).

Anal. Calcd for $C_{15}H_{25}N_2O_3WCl$: C, 35.98; H, 5.03; N, 5.59. Found: C, 36.20; H, 5.06; N, 5.35. IR (Nujol mull): ν_{CO_2} 1616 (s) and 1591 (s), ν_{NO} 1566 (s) cm^{-1}. ^1H NMR ($CDCl_3$): δ 5.0 (s, 1H, N*H*), 2.01 (s, 15H, C_5Me_5), 1.36 (s, 9H, CMe_3). $^{13}C\{^1H\}$ NMR ($CDCl_3$): δ 164.70 (*OCO*), 115.78 (C_5Me_5), 51.29 ($NHCMe_3$), 29.28 ($NHCMe_3$), 9.62 (C_5Me_5). Low-resolution mass spectrum (probe temperature 200 °C): *m/z* 502 [P^+].

Kinetic Study of the Reaction between Complex 2 and *p*-Tolyl Isocyanate. All experiments were performed similarly in J. Young thin-walled NMR tubes equipped with Teflon stoppers. The following procedure is representative. In a glovebox, complex 2 (30 mg, 0.061 mmol), Cp_2Fe (5.0 mg, 0.027 mmol), and the desired amount of *p*-tolyl isocyanate were introduced into the NMR tube. An amount of C_6D_6 to make the volume up to 0.78 mL was added to this mixture. The contents of the tubes were then degassed and stored at −30 °C until needed. For each experiment, the tube and its contents were placed into a NMR probe warmed to 55 °C. The tube was allowed to equilibrate to the probe temperature over a period of 3 min. All reactions were monitored by ^1H NMR spectroscopy at 55 °C by integrating the resonance of the upfield *tert*-butyl group of product 6 versus that of the ferrocene standard. For each data point, two spectra were recorded 1 min apart, each with a single acquisition. Each spectrum was integrated separately and

Table 1. Crystallographic Data for Cp*W(NO)(η^2-C{NCMe$_3$}CH$_2$CMe$_3$)(OCMe$_3$) (5)[a]

compd	Cp*W(NO)(η^2-C{NCMe$_3$}CH$_2$CMe$_3$)(OCMe$_3$), **5**
formula	$C_{24}H_{44}N_2O_2W$
fw	576.47
color, habit	yellow, prism
cryst size, mm	0.40 × 0.40 × 0.45
cryst syst	orthorhombic
space group	*Pbca*
a, Å	17.459(2)
b, Å	20.3939(3)
c, Å	15.075(3)
V, Å^3	5367(1)
Z	8
ρ_{calc}, g/cm^3	1.427
F(000)	2336
radiation	Mo
μ, cm^{-1}	43.28
transmissn factors (rel)	0.84–1.00
scan type	ω–2θ
scan range, deg in ω	1.15 ± 0.35 tan θ
scan speed, deg/min	32
data collected	$+h,+k,+l$
$2\theta_{max}$, deg	65
cryst decay, %	negligible
total no. of unique reflections	10520
no. of reflections with $I \geq 3\sigma(I)$	3856
no. of variables	263
R	0.032
R_w	0.027
GOF	1.48
max Δ/σ (final cycle)	0.02
residual density, e/Å^3	–0.95, 0.53 (both near W)

[a] Temperature 294 K, Rigaku AFC6S diffractometer, Mo K$_\alpha$ (λ = 0.71069 Å) radiation, graphite monochromator, takeoff angle 6.0°, aperture 6.0 × 6.0 mm at a distance of 285 mm from the crystal, stationary background counts at each end of the scan (scan/background time ratio 2:1), $\sigma^2(F^2) = [S^2(C + 4B)]/Lp^2$ (S = scan rate, C = scan count, B = normalized background count), function minimized $\sum w(|F_o| - |F_c|)^2$ where $w = 4F_o^2/\sigma^2(F_o^2)$, $R = \sum||F_o| - F_c||/\sum|F_o|$, $R_w = (\sum w(|F_o| - |F_c|)^2/\sum w|F_o|^2)^{1/2}$, and GOF = $[\sum w(|F_o| - |F_c|)^2/(m - n)]^{1/2}$. Values given for R, R_w, and GOF are based on those reflections with $I \geq 3\sigma(I)$.

averaged for each data point. All first-order plots of $-\ln([6]_\infty - [6]_t)$ vs time displayed linearity over at least 2 half-lives with $r^2 \geq 0.98$.

X-ray Crystallographic Analysis of Cp*W(NO)(η^2-C{NCMe$_3$}CH$_2$CMe$_3$)(OCMe$_3$) (5). Crystallographic data appear in Table 1. The final unit-cell parameters were obtained by least-squares on the setting angles for 25 reflections with 2θ = 39.3–41.7°. The intensities of three standard reflections, measured every 200 reflections throughout the data collection, remained constant. The data were processed[11] and corrected for Lorentz and polarization effects, and absorption (empirical, based on azimuthal scans for three reflections).

The structure was solved by conventional heavy atom methods, the coordinates of the tungsten atom being determined from the Patterson function and those of the remaining non-hydrogen atoms from subsequent difference Fourier syntheses. All non-hydrogen atoms were refined with anisotropic thermal parameters. Hydrogen atoms were fixed in idealized positions (methyl group orientations based on observed difference map peaks) with C–H = 0.99 Å and $B_H = 1.2B_{\text{bonded atom}}$. A correction for secondary extinction was applied, the final value of the extinction coefficient being [1.27(3)] × 10^{-7}. Neutral atom scattering factors[12a] for all atoms and anomalous dispersion corrections for the non-hydrogen atoms[12b] were taken from the *International Tables for X-Ray Crystallography*. Final positional and equivalent isotropic thermal parameters for the complex are given in Table 2, and selected bond lengths (Å) and bond angles (deg) are listed in Table 3. A view of the solid-state molecular structure of complex **5** is displayed in Figure 1. Hydrogen atom parameters, anisotropic thermal parameters, complete tables of bond lengths and angles, torsion angles, intermolecular contacts, and least-squares planes are included as supplementary material.

(11) *teXsan*: Crystal Structure Analysis Package, Molecular Structure Corp., 1985 & 1992.

(12) (a) *International Tables for X-Ray Crystallography*; Kynoch Press: Birmingham, U.K., 1974; Vol. IV, pp 99–102. (b) *International Tables for X-Ray Crystallography*; Kluwer Academic Publishers: Boston, 1992; Vol. C, pp 219–222.

Table 2. Final Positional and Equivalent Isotropic Thermal Parameters (Å^2) for Cp*W(NO)(η^2-C{NCMe$_3$}CH$_2$CMe$_3$)(OCMe$_3$) (5)

atom	*x*	*y*	*z*	B_{eq}[a]
W(1)	0.21792(1)	0.16718(1)	0.11836(1)	2.725(4)
O(1)	0.1730(3)	0.2334(2)	0.2870(2)	5.4(1)
O(2)	0.1965(2)	0.0749(2)	0.1504(2)	3.88(9)
N(1)	0.1865(3)	0.2042(2)	0.2177(3)	3.3(1)
N(2)	0.1302(2)	0.1570(2)	0.0179(3)	3.5(1)
C(1)	0.3128(3)	0.2218(3)	0.0301(4)	3.2(1)
C(2)	0.3185(3)	0.1552(3)	0.0051(4)	3.8(1)
C(3)	0.3406(3)	0.1191(3)	0.0777(4)	4.2(2)
C(4)	0.3479(3)	0.1625(3)	0.1526(4)	3.9(1)
C(5)	0.3318(3)	0.2260(3)	0.1209(4)	3.7(1)
C(6)	0.3010(3)	0.2796(3)	–0.0323(4)	5.1(2)
C(7)	0.3040(4)	0.1310(4)	–0.0884(4)	5.8(2)
C(8)	0.3530(4)	0.0458(3)	0.0797(5)	6.9(2)
C(9)	0.3792(4)	0.1466(4)	0.2408(4)	6.3(2)
C(10)	0.3418(4)	0.2895(3)	0.1736(4)	5.3(2)
C(11)	0.1615(4)	0.0451(3)	0.2274(4)	4.7(2)
C(12)	0.2100(4)	0.0580(3)	0.3099(4)	6.5(2)
C(13)	0.0819(4)	0.0708(4)	0.2411(5)	7.2(2)
C(14)	0.1600(5)	–0.0284(3)	0.2082(4)	6.9(2)
C(15)	0.1426(3)	0.2174(3)	0.0331(3)	3.0(1)
C(16)	0.1027(3)	0.2776(3)	–0.0007(4)	3.8(1)
C(17)	0.0761(3)	0.3277(3)	0.0684(4)	3.8(1)
C(18)	0.1438(4)	0.3575(3)	0.1168(4)	4.7(1)
C(19)	0.321(4)	0.3809(3)	0.0185(4)	5.4(2)
C(20)	0.226(3)	0.2957(3)	0.1340(4)	5.3(2)
C(21)	0.0710(3)	0.1204(3)	–0.0349(4)	4.0(1)
C(22)	0.0732(4)	0.1433(3)	–0.1316(4)	6.2(2)
C(23)	–0.0066(4)	0.1301(3)	0.0063(5)	5.5(2)
C(24)	0.0948(4)	0.0489(3)	–0.0321(4)	5.6(2)

[a] $B_{eq} = 8/3\pi^2(U_{11}(aa^*)^2 + U_{33}(bb^*)^2 + 2U_{12}aa^*bb^* \cos\gamma + 2U_{13}aa^*cc^* \cos\beta + 2U_{23}bb^*cc^* \cos\alpha)$.

Table 3. Selected Metrical Parameters[a] for Cp*W(NO)(η^2-C{NCMe$_3$}CH$_2$CMe$_3$)(OCMe$_3$) (5)

Bond Lengths (Å)			
W(1)–CP[b]	2.07	W(1)–N(1)	1.765(4)
W(1)–O(2)	1.978(4)	N(2)–C(15)	1.271(6)
W(1)–N(2)	2.164(4)	O(1)–N(1)	1.224(5)
W(1)–C(15)	2.104(5)		
Bond Angles (deg)			
O(2)–W(1)–N(1)	98.1(2)	N(2)–W(1)–C(15)	34.6(2)
O(2)–W(1)–N(2)	86.9(2)	W(1)–O(2)–C(11)	132.5(2)
O(2)–W(1)–C(15)	119.6(2)	W(1)–N(1)–O(1)	172.5(5)
N(1)–W(1)–N(2)	114.5(2)	W(1)–N(2)–C(15)	70.1(3)
N(1)–W(1)–C(15)	96.6(2)	W(1)–C(15)–N(2)	75.3(3)

[a] ESD's in parentheses. [b] CP refers to the unweighted centroid of the cyclopentadienyl ligand.

Results

The reactivities of each of the complexes **1**, **2**, and **3** with *tert*-butyl isocyanide, *p*-tolyl isocyanate, and carbon disulfide are summarized in Schemes 1, 2, and 3.

Insertions of *tert*-Butyl Isocyanide (Scheme 1). The reaction of complex **1** in C_6D_6 with excess *tert*-butyl isocyanide does not proceed at any appreciable rate in the temperature range 20–70 °C. However, when the reaction is carried out in $CDCl_3$ at 70 °C, the complex Cp*W(NO)(η^2-C{NCMe$_3$}CH$_2$CMe$_3$)Cl (**4**), is produced. The ^{13}C NMR spectrum of this complex in $CDCl_3$ reveals that the signal at δ 41.66 ppm assignable to the neopentyl group no longer bears satellites due to ^{183}W (14% natural

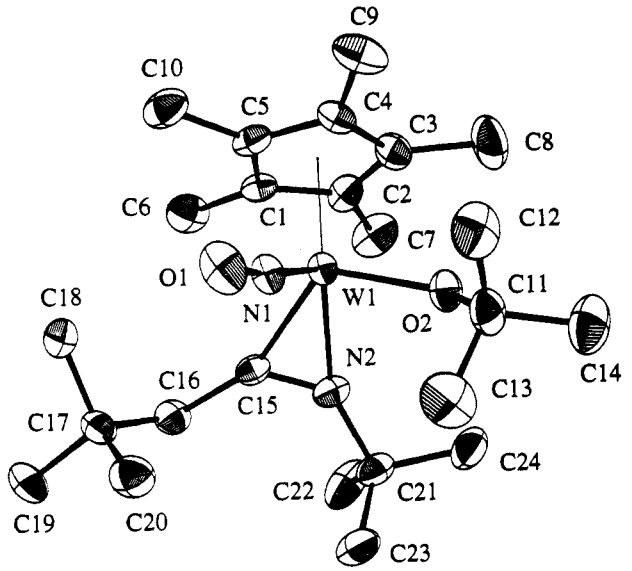

Figure 1. ORTEP diagram of $Cp^*W(NO)(\eta^2\text{-}C\{NCMe_3\}CH_2CMe_3)(OCMe_3)$ (**5**). Probability ellipsoids at the 33% level are shown; hydrogen atoms have been omitted for clarity.

Scheme 1

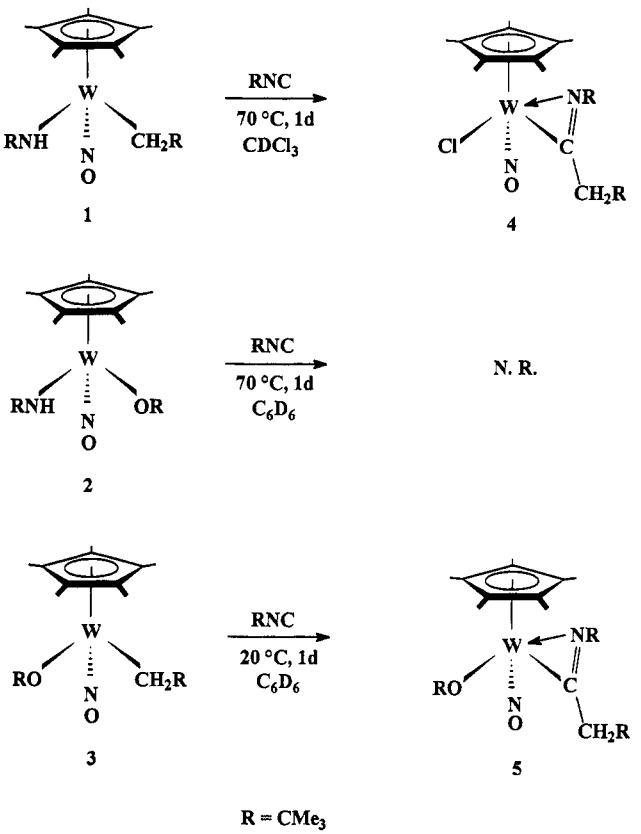

abundance). Also, the ^1H NMR spectrum of **4** exhibits two doublets at δ 3.54 and 2.85 ppm assignable to the diastereotopic methylene protons of the neopentyl group. These large downfield shifts from δ 1.15 and 1.01 ppm of the resonances due to the methylene protons of complex **1** also indicate that insertion of the isocyanide into the W–C bond has occurred. Thermolysis of **1** in $CDCl_3$ in the absence of *tert*-butyl isocyanide results in only slight decomposition of **1**. Consequently, the loss of the amide group during the formation of **4** most likely occurs with involvement of the $CDCl_3$ solvent to afford the chloro ligand *after* the insertion has occurred.

Scheme 2

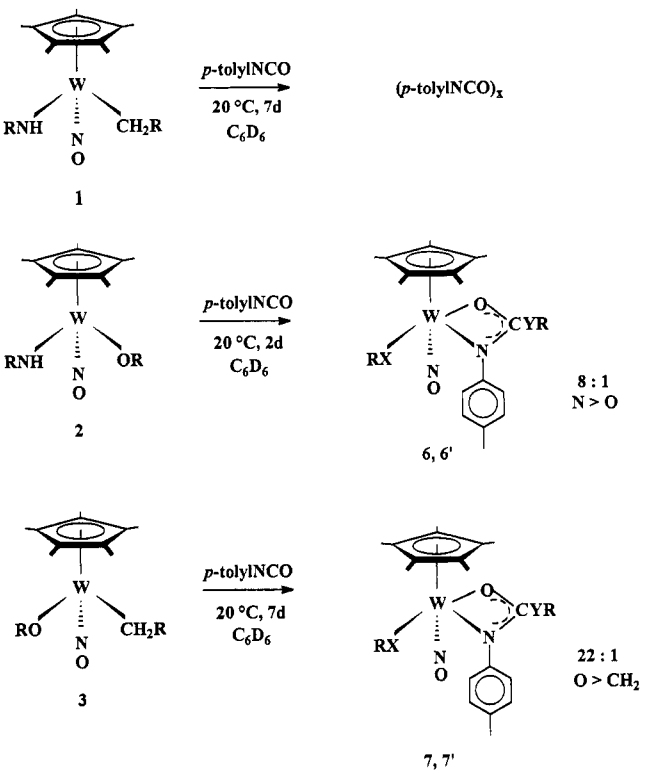

R = CMe_3; X, Y = CH_2 or NH or O

Treatment of complex **2** with excess *tert*-butyl isocyanide even at 100 °C does not result in a reaction, and longer reaction times or higher temperatures result in decomposition of the organometallic starting material. However, the analogous reaction of complex **3** with excess *tert*-butyl isocyanide proceeds cleanly at 20 °C and affords the one product complex, **5**. Again, just as for complex **1** (vide supra), the spectroscopic properties of the product complex indicate that the isocyanide insertion has occurred into the W–C bond. The Nujol mull IR spectra of **4** and **5** exhibit characteristic $\nu_{C=N}$ absorptions at 1680 and 1637 cm^{-1} in the range expected for η^2-iminoacyls.[13] The existence of this ligand has been confirmed by a single-crystal X-ray crystallographic analysis of complex **5**.

X-ray Analysis of Complex 5. This analysis confirms that insertion of *tert*-butyl isocyanide had occurred into the W–C bond of **3** and that the resulting iminoacyl ligand is bound in an η^2-fashion to the metal center (Figure 1). The intramolecular metrical parameters of **5** are comparable to those found for related 18-valence-electron pianostool molecules.[5] The W–C and W–N bond lengths in **5** of 2.104(5) and 2.164(4) Å, respectively, are quite similar to those found for $CpMo(CO)_2(\eta^2\text{-}C\{NPh\}Me)$ which are 2.106(5) and 2.143(4) Å,[14] respectively. The W–O bond length of 1.978(4) Å in **5** is significantly longer than that (1.916(4) Å) extant in the related complex $Cp^*W(NO)(OCMe_3)(NHCMe_3)$.[7] This lengthening may well be reflective of decreased M–O π-bonding in **5** which is the result of a more electron-rich tungsten center.

Insertions of *p*-Tolyl Isocyanate (Scheme 2). Exposure of complex **1** to excess *p*-tolyl isocyanate does not result in isolable insertion products, but rather affords the polymer of the isocyanate reagent, $(p\text{-}Me\text{-}C_6H_4NCO)_x$,

(13) Durfee, L. D.; Rothwell, I. P. *Chem. Rev.* **1988**, *88*, 1059.
(14) Adams, R. D.; Chodosh, D. F. *Inorg. Chem.* **1978**, *17*, 41.

Table 4. Rate Constants for the Reaction of Cp*W(NO)(OCMe$_3$)(NHCMe$_3$) (2) with *p*-Tolyl Isocyanate[a]

[isocyanate], M	equiv of isocyanate	k_{obs} ($\times 10^5$ s)[b]	k_2 ($\times 10^5$ M s)
0.79	10	1.2(4)	1.5
1.58	20	2.7(5)	1.7
2.37	30	4.3(6)	1.8
3.16	40	6.2(9)	2.0

[a] All reactions carried out in C_6D_6 at 55°C and [2] = 7.9×10^{-2} M. [b] Errors estimated from reproducibility of runs.

as a white powder. In contrast, complex **2** reacts with excess *p*-tolyl isocyanate and produces two product complexes, **6** and **6′**, in a ratio of 8:1 as determined by ^{1}H NMR spectroscopic monitoring. In the ^{13}C NMR spectrum of the major insertion product **6** in C_6D_6, the peaks attributable to the quaternary carbons of the OCMe$_3$ and NCMe$_3$ groups appear at δ 81.28 and 50.99 ppm, respectively. The large upfield shift of approximately 10 ppm (as compared to complex **2**) in the resonance attributable to the quaternary carbon of the NCMe$_3$ group indicates that the major product has resulted from isocyanate insertion into the W–N and not the W–O bond. The minor product is thus assigned to result from the analogous insertion into the W–O bond.

When complex **3** is treated with excess *p*-tolyl isocyanate, the two complexes **7** and **7′** are produced in the approximate ratio of 22:1. The ^{13}C NMR spectrum of the insertion products reveals that the peak assignable to the methylene carbon of the neopentyl ligand has satellites due to ^{183}W ($^1J_{WC}$ = 78 Hz). Thus, the major product **7** must result from insertion into the W–O bond since the neopentyl ligand remains bound to tungsten. The minor product **7′**, therefore, results from the insertion of the isocyanate into the W–C bond.

The η^2-nature of the isocyanate-inserted ligands is indicated by the diagnostic ν_{CO} stretch of the N-bound ligand evident in the IR spectra of the complexes. Both of the insertion products **6** and **7** have features in their Nujol-mull IR spectra (1556 and 1538 cm^{-1}, respectively) consistent with η^2 attachment of the isocyanate-inserted ligand.[15] Furthermore, the fact that these values of ν_{CO} in **6** and **7** are approximately 100 cm^{-1} lower in energy than that for the free urea is consistent with C–O–M coordination of the ligand. This in turn implies that isocyanate insertion has occurred into the W–N bond of **2** and not in the N–H bond as has been observed previously during the reactions of isocyanates with some organic amines[16] and some late transition-metal amide complexes.[17]

Kinetic Study of the *p*-Tolyl Isocyanate Insertion into Complex 2. The reaction of complex **2** with excess *p*-tolyl isocyanate can be conveniently studied by ^{1}H NMR spectroscopy at 55 °C. This investigation has established that the reaction is first order in complex **2** under the experimental conditions employed, the observed rate constants being listed in Table 4. These rate constants are linearly dependent on the concentration of isocyanate, the plots of $-\ln([6]_\infty - [6]_t)$ vs t being shown in Figure 2,

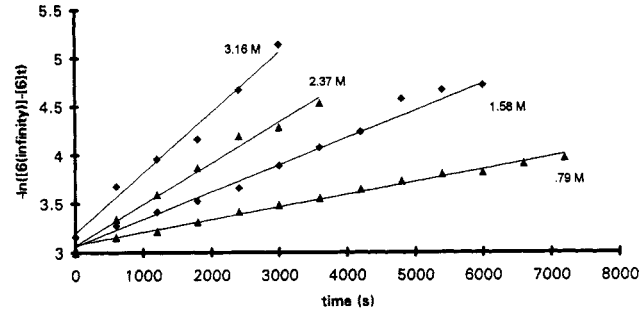

Figure 2. Plots of $-\ln([6]_\infty - [6]_t)$ vs t. Concentrations of *p*-tolyl isocyanate are indicated for each run.

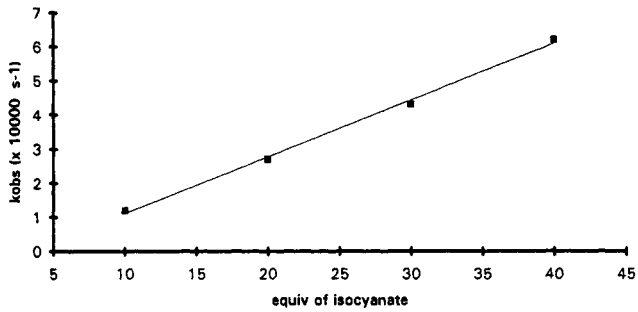

Figure 3. Plot of k_{obs} vs equiv of isocyanate.

Scheme 3

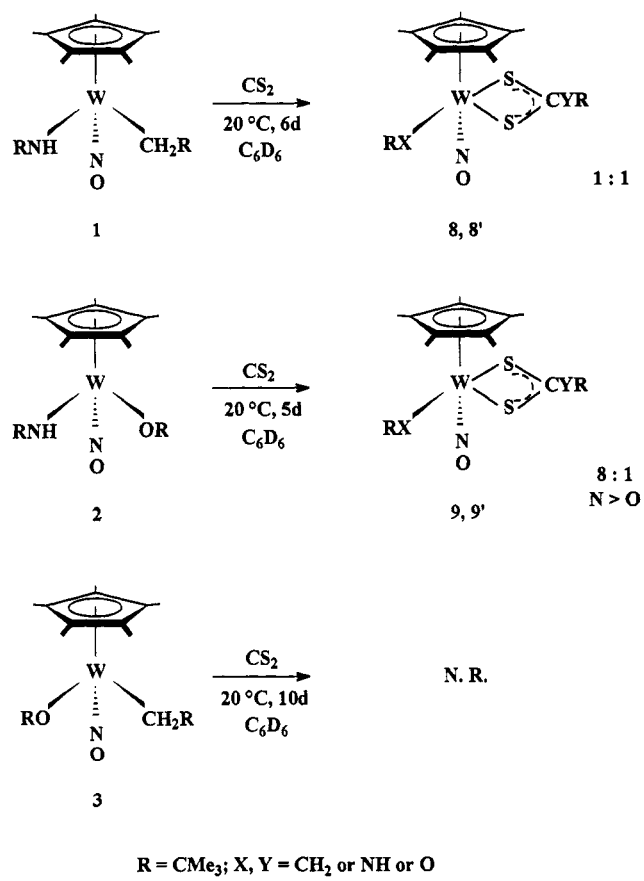

and the plot of k_{obs} vs [*p*-tolyl isocyanate] being shown in Figure 3.

Insertions of Carbon Disulfide (Scheme 3). When complex **1**, Cp*W(NO)(CH$_2$CMe$_3$)(NHCMe$_3$), is treated with excess CS_2 at ambient temperatures for 6 d, ^{1}H NMR spectroscopy reveals that two complexes, **8** and **8′**, are cleanly produced in a 1:1 ratio. These two products result from CS_2 insertion into the W–C and the W–N bonds,

(15) See, for example: (a) Lam, H.; Wilkinson, G.; Hussain-Bates, B.; Hursthouse, M. B. *J. Chem. Soc., Dalton Trans.* **1993**, 781. (b) Leung, W.-H.; Wilkinson, G.; Hussain-Bates, B.; Hursthouse, M. B. *J. Chem. Soc., Dalton Trans.* **1991**, *2791*.

(16) March, J. *Advanced Organic Chemistry*; Academic Press: New York, 1985; Ch 6.

(17) Glueck, D. S.; Newman Winslow, L. J.; Bergman, R. G. *Organometallics* **1991**, *10*, 1462.

respectively, a conclusion easily substantiated by ^{13}C NMR spectroscopy. Thus, the signal assignable to the methylene carbon (δ 52.58 ppm) of complex **8** in C_6D_6 does not have ^{183}W satellites, whereas the analogous peak due to complex **8′** (δ 51.24 ppm) does ($^1J_{WC}$ = 73 Hz). No attempt has been made to separate these two insertion products.

Similarly, treatment of **2**, Cp*W(NO)(OCMe$_3$)(NHCMe$_3$), with excess CS_2 at room temperature produces **9** and **9′** in the approximate ratio of 8:1. Again, the site of insertion in these products can be assigned on the basis of comparative ^{13}C NMR spectroscopy. In the ^{13}C NMR spectrum of reactant **2** in C_6D_6 there are two peaks assignable to the quaternary carbons of the OCMe$_3$ group (δ 79.21 ppm) and the NCMe$_3$ group (δ 61.11 ppm) and two peaks at higher field attributable to the methyl groups of the two *tert*-butyl groups (δ 34.43 and 33.51 ppm). These chemical shift values for the signals due to the quaternary carbons of the *tert*-butyl groups are comparable to those in the spectra of Cp*W(NO)(OCMe$_3$)Cl[18] and Cp*W(NO)(NHCMe$_3$)Cl[7] which appear at δ 85.20 and 65.04 ppm, respectively. For comparison, the ^{13}C NMR spectrum of the major insertion product **9** displays peaks assignable to the quaternary carbons of the OCMe$_3$ and NCMe$_3$ groups at δ 78.32 and 56.31 ppm, respectively. As well, the peaks assignable to the methyl groups of the *tert*-butyl groups appear at δ 34.28 (OC*Me*$_3$) and 28.34 (NC*Me*$_3$) ppm. These large upfield shifts of approximately 5 ppm in the ^{13}C resonances attributable to the NCMe$_3$ group indicate that the major product results from CS_2 insertion into the W–N bond and not the W–O bond. The minor product is thus assigned to result from insertion of CS_2 into the W–O bond.

The CS_2 insertion products are formulated as having η^2-S_2CR ligands on the basis of their Nujol-mull IR spectra. For example, the spectrum of complex **9** reveals two bands at 1178 and 1022 cm^{-1} which are assignable to the symmetric and asymmetric stretching frequencies of the CS_2-containing fragment. These values are comparable to those exhibited by the related CS_2-inserted product, Cp*W(NO)(η^2-S_2CPh)(Ph), which exhibits two bands in its IR spectrum at 1176 and 1021 cm^{-1}.[19]

Finally, complex **3** does not react with excess CS_2 in C_6D_6 or $CDCl_3$ in the temperature range 20–80 °C over a period of 1 week. Higher temperatures result in the thermal decomposition of the starting material to many products.

Reactions with Carbon Dioxide. The outcomes of the reactions of complexes **1–3** with CO_2 are not as straightforward as those discussed above. When a C_6D_6 solution of **1** is treated with 15 psi CO_2, there is a clean conversion to the insertion product for which ^{13}C NMR spectroscopy indicates that the insertion of CO_2 into the W–N bond has occurred. Thus, the resonance attributable to the methylene carbon of the product still bears satellites due to coupling to the tungsten center ($^1J_{WC}$ = 81 Hz). All spectroscopic and analytical data are consistent with the product being the CO_2-inserted complex, Cp*W(NO)(η^2-O_2CNHCMe$_3$)(CH$_2$CMe$_3$) (**10**) (eq 1). In contrast, when the analogous reaction between **2** and CO_2 is monitored by ^1H NMR spectroscopy, a final reaction mixture consisting of three major Cp*-containing products is

$$\text{Cp*W(NO)(CH}_2\text{CMe}_3\text{)(NHCMe}_3\text{)} + CO_2 \rightarrow \text{Cp*W(NO)}(\eta^2\text{-O}_2\text{CNHCMe}_3\text{)(CH}_2\text{CMe}_3\text{)} \quad (1)$$

revealed. Mass spectrometric analysis of this mixture reveals signals attributable to a mono-inserted species, **11**, as well as higher molecular weight species. Attempts to separate these products by column chromatography and fractional crystallization have to date been unsuccessful. Treatment of complex **2** with CO_2 at 80 °C again produces a mixture of products, but in this case an organic product can be isolated. On the basis of its IR, NMR, and mass spectral properties, this product has been identified as (Me$_3$CNH)$_2$CO, and it is probably formed by incorporation of CO_2 into the W–N bond of **2** followed by subsequent decomposition of the resulting organometallic complex. This organic compound can also be obtained by the reaction of the free amine with CO_2 or CO in the presence of selenium.[20] Finally, it may be noted that complex **3** does not react with CO_2 under similar experimental conditions.

The reactivity studies with CO_2 have been extended to the simpler amido chloro, alkyl chloro, and alkoxo chloro complexes, Cp*W(NO)(XCMe$_3$)Cl (X = NH, CH$_2$, and O). Of these three complexes, the only compound that reacts with 15 psi CO_2 is the amido chloro complex, Cp*W(NO)(NHCMe$_3$)Cl, which cleanly converts to the mono-inserted species, Cp*W(NO)(η^2-O_2CNHCMe$_3$)Cl (**12**). Similar facile insertion of CO_2 into M–N bonds has been observed for other systems.[6,21]

Discussion

The ability of a reagent to react in a regioselective manner is of paramount importance in all types of synthetic chemistry. The three complexes **1–3** have pairs of ligands which differ only in the moieties α to the metal, namely NH/CH$_2$ (**1**), NH/O (**2**), and CH$_2$/O (**3**). These pairings of ligands allow comparative inter- and intramolecular reactivity studies involving these bonds. To the best of our knowledge, our investigations in this regard are unique in that all previous comparative bond reactivity studies have involved ligands with different steric properties or have effected only intermolecular (as opposed to intramolecular) comparisons.[6] We begin our discussion by a consideration of the insertion preferences of the various linkages toward the three substrates employed.

The reactions of complexes **1–3** with *tert*-butyl isocyanide (Scheme 1) indicate that the only site of insertion in these compounds is the W–C bond, the W–N and W–O linkages being unreactive with *tert*-butyl isocyanide. This finding is consistent with those of other studies which have also found that M–C linkages preferentially insert isocyanides.[22] For example, the M–C bonds in Cp*$_2$U(NEt$_2$)(Me)[23] and Cp$_2$Zr(OAr)CH$_2$Ph (OAr = 2-methyl-6-*tert*-butylphenoxide)[24] are the insertion sites rather than

(18) Legzdins, P.; Lundmark, P. J.; Rettig, S. J. *Organometallics* **1993**, *12*, 3545.
(19) Brouwer, E. B.; Legzdins, P.; Rettig, S. J.; Ross, K. J. *Organometallics* **1993**, *12*, 4234.
(20) Sonoda, N.; Yasuhara, T.; Kondo, K.; Ikeda, T.; Tsutsumi, S. *J. Am. Chem. Soc.* **1971**, *93*, 6344.
(21) (A) Chisholm, M. H.; Rothwell, I. P. *Comprehensive Coordination Chemistry*; Pergamon: New York, 1987; Vol. 2, pp 161–188. (b) Chisholm, M. H.; Cotton, F. A.; Extine, M. W.; Reichert, W. W. *J. Am. Chem. Soc.* **1978**, *100*, 1727.
(22) Klein, D. P.; Hayes, J. C.; Bergman, R. G. *J. Am. Chem. Soc.* **1988**, *110*, 3704.
(23) Zanella, P.; Brianese, N.; Casellato, U.; Ossala, F.; Porchin, M.; Rossetto, G.; Graziani, R. *J. Chem. Soc., Dalton Trans.* **1987**, 2039.
(24) Chamberlain, L. R.; Durfee, L. D.; Fanwick, P. E.; Kobriger, L.; Latesky, S. L.; McMullen, A. K.; Rothwell, I. P.; Folting, K.; Huffman, J. C.; Streib, W. E.; Wang, R. *J. Am. Chem. Soc.* **1987**, *109*, 390.

Scheme 4

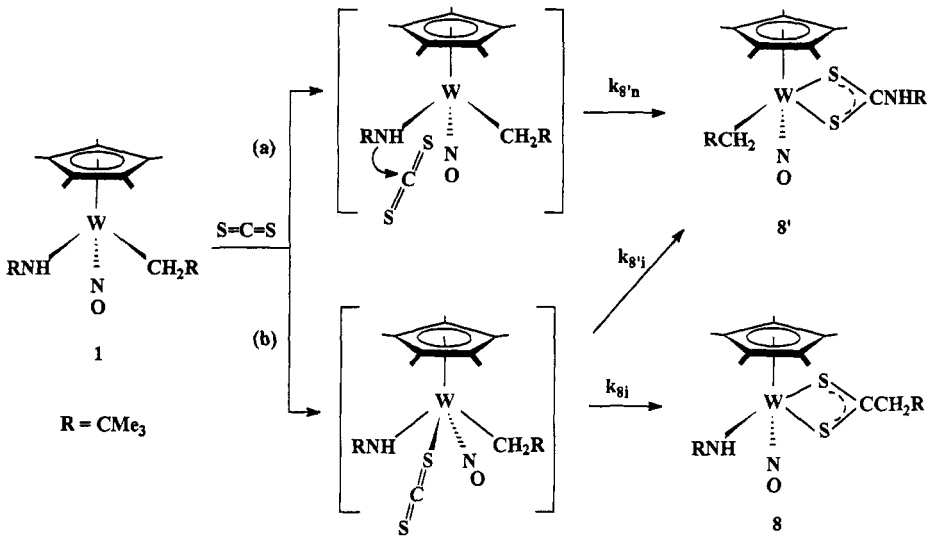

the M–N and M–O bonds, respectively, in the two complexes. The lack of reactivity of complex **2** toward *tert*-butyl isocyanide is not surprising given that complex **2** does not form an adduct with PMe_3 at room temperature thereby indicating that the metal center is relatively electron sufficient.[7] These observations are consistent with a mechanism which involves initial adduct formation followed by migration/insertion into the weakest M–X linkage (vide infra).

The reactions of **1–3** with *p*-tolyl isocyanate (Scheme 2) establish that the preferential site of insertion in these compounds is W–N > W–O > W–C. This trend may reflect the higher nucleophilicities of the amide nitrogen and the alkoxide oxygen atoms over the methylene carbon atom of the alkyl group. This polymerization of the isocyanate effected by complex **1** is somewhat surprising given that complexes **2** and **3**, with very similar ligand systems, undergo insertion, and polymerization of the isocyanate does not occur. This preferential polymerization probably indicates that the initial insertion product is unstable to further insertion of the isocyanate. The reactivity trend observed with complexes **1–3** parallels a related study in which the comparative reactivity of phenyl isocyanate with both hydride and amide functionalities at the same metal center was studied and insertion was found to occur exclusively into the M–N bond,[25] i.e. eq 2.

$$trans\text{-(H)Pt(NHPh)(PEt}_3)_2 + \text{PhNCO} \rightarrow trans\text{-(H)Pt(N\{Ph\}C\{O\}NHPh)(PEt}_3) \quad (2)$$

Carbon disulfide reacts with **1** to form the inserted complexes **8** and **8'** in the ratio of 1:1 (Scheme 3). This observation indicates that there is no overall preferential site of insertion of CS_2 into complex **1**. This clean insertion of CS_2 into the M–C and M–N bonds of complex **1** is in contrast to the reaction between CS_2 and the $[W(CO)_5Me]^-$ anion which occurs with significant concomitant decomposition.[26] With **2**, the preferential site of CS_2 reactivity is the W–N bond over the W–O bond by a ratio of 8:1. On the basis of these results, it might have been expected that complex **3** should yield two products in the ratio of 8:1 with the major product resulting from insertion of CS_2 into the W–C bond. Interestingly, **3** is unreactive with CS_2 even at elevated temperatures. This fact indicates that the outcome of the reaction is not solely dependent on the availability of a bond that can undergo insertion, but it is also dependent on the electronic nature of the molecule given that the steric nature of complexes **1–3** is quite similar. Nevertheless, the preferential site of insertion of CS_2 into this series of complexes is W–N ≅ W–C > W–O. Consistently, the only complexes of this type that we have found to react with CO_2 are those that contain W–N linkages, again confirming the increased nucleophilicity of the amido nitrogen. In closing this section, it may be noted that insertion of CS_2 also occurs preferentially into the Ir-heteroatom bond of the complexes $Cp^*Ir(PPh_3)(XR)(H)$ where XR = arylamide or alkoxide.[17]

Mechanistic Considerations. The outcomes of the reactions investigated during this study are best rationalized in terms of two distinct mechanisms operating simultaneously. These mechanisms are illustrated in Scheme 4 for the reaction of complex **1** with CS_2 to produce **8** and **8'** and involve (a) direct nucleophilic attack on CS_2 by the amido ligand of **1** to produce **8'** and (b) initial coordination of CS_2 to the tungsten center followed by insertion of CS_2 into the metal–alkyl or metal–amido linkages to produce **8** or **8'**, respectively. The rate constants indicated in Scheme 4 are those for the overall formation of the specific products, e.g. k_{8i} is the overall rate constant for the formation of **8** via the insertion path, etc. Since the experimentally determined ratio of **8**:**8'** is 1:1, it follows that the rate of insertion of the alkyl group is at least as fast as insertion of the amide (i.e. $k_{8i} \geq k_{8'i}$) because k_{8n} is most likely not zero (i = insertion, n = nucleophilic attack).

The reaction of complexes **1–3** with *tert*-butyl isocyanide can be rationalized in a similar manner. Complexes **1** and **3** afford the mono-inserted products **8** and **9**, but **2** displays no reactivity with *tert*-butyl isocyanide under similar experimental conditions. Since complex **2** does form insertion products with CS_2 and *p*-tolyl isocyanate, this lack of reactivity with *tert*-butyl isocyanide indicates that the successful insertions most likely proceed by intermolecular nucleophilic attack on the heterocumulenes (mechanistic path a). Consistent with the view that complex **2** does not react with heterocumulenes via path b is the fact that the metal center in **2** does not form an adduct even

(25) Cowan, R. L.; Trogler, W. C. *J. Am. Chem. Soc.* **1989**, *111*, 4750.
(26) Darensbourg, D. J.; Wiegreffe, H. P.; Reibenspies, J. H. *Organometallic* **1991**, *10*, 6.

with the strong Lewis base PMe_3. In other words, **2** is simply too weak a Lewis acid to follow path b. Monitoring of the reaction between **3** and *tert*-butyl isocyanide by ^1H NMR spectroscopy does reveal signals that may be attributed to an initial Lewis acid–Lewis base adduct [i.e. δ 1.80 (C_5Me_5), 1.42, 1.25, 1.03 ($3 \times CMe_3$) ppm] in which the isocyanide probably occupies the coordination position between the nitrosyl and the alkoxide ligands in which it is least likely to undergo insertion into the W–C bond. Regrettably, all attempts to isolate this adduct to date have been unsuccessful.

Consistent with the mechanistic interpretation outlined in the preceding two paragraphs, the outcomes of the reactions between complexes **1**–**3** and the heterocumulene, *p*-tolyl isocyanate, indicate that intermolecular nucleophilic attack via path a is the predominant reaction pathway. Kinetic evidence regarding path a has been obtained by monitoring the reaction of complex **2** with excess *p*-tolyl isocyanate (vide supra). This monitoring indicates that the insertion reaction proceeds via simple bimolecular reaction. The conversion of complex **2** to complexes **6** and **6′** can be viewed as parallel path a reactions which require the $k_6/k_{6'}$ = [**6**]/[**6′**] at any time of the conversion.[27] Since the ratio of **6**:**6′** is 8:1 then $k_6/k_{6'}$ = 8/1. Figure 3 yields k_2 = slope = $2(1) \times 10^{-5}$ M^{-1} s^{-1}, and thus $k_6 \approx 2 \times 10^{-5}$ M^{-1} s^{-1} and $k_{6'} \approx 2 \times 10^{-6}$ M^{-1} s^{-1}. The insertion of CS_2 into an Re–O linkage has also been found to be consistent with a simple bimolecular process.[28]

In closing, the mechanisms involved in the insertion of heterocumulenes into metal–heteroatom and metal–carbon bonds have not yet been fully elucidated. As noted above, the insertion of CS_2 into a metal–oxygen bond has been determined to occur by nucleophilic attack at the central carbon of the heterocumulene.[28] There is less information with regard to the mechanism of insertion into metal–alkyl bonds. For example, the neutral Re(I) alkyls $(CO)_5ReR$ react with CS_2 to afford the complexes $(CO)_4Re(\eta^2\text{-}S_2CR)$,[29] but the mechanism of these transformations is unclear. Nevertheless, there is little likelihood that the insertion of a heterocumulene into a metal–alkyl bond would occur by nucleophilic attack at the heterocumulene by the alkyl ligand without the initial formation of a metal-centered adduct.

Epilogue

In general, this work has established the insertion preference for a metal–heteroatom linkage over that of a metal–alkyl bond for heterocumulene insertion. In contrast, the metal–alkyl linkage is the preferred site of insertion for *tert*-butyl isocyanide. Since the insertion of CO, a valence-isoelectronic analogue of *tert*-butyl isocyanide, into metal–alkyl bonds generally proceeds via initial adduct formation at the metal center followed by alkyl migration,[30] it would be expected that intramolecular migration of an alkyl group would occur preferentially to that of an amide or alkoxide ligand especially where the possibility of multiple bonding of these latter ligands to th e unsaturated metal center exists (as it does for the formally 16-valence-electron complexes studied in this work). This predicted insertion preference of *tert*-butyl isocyanide for metal–alkyl over metal–amide or –alkoxide linkages has been confirmed experimentally. This work has also established that heterocumulene insertions evidently proceed via intermolecular nucleophilic attack, and hence the insertion preference is dominated by the nucleophilicity of the ligand undergoing the insertion. Hopefully, the results of these investigations, along with those of others, will assist in the future development of rational syntheses of increasingly complex organometallic compounds by exploiting the knowledge of the most probable sites of competitive reactivity of particular substrates.

Acknowledgment. We are grateful to the Natural Sciences and Engineering Research Council of Canada for support of this work in the form of grants to P.L. and a postgraduate scholarship to K.J.R.

Supplementary Material Available: Tables of hydrogen-atom parameters, anisotropic thermal parameters, complete listings of bond lengths and bond angles, torsion angles, intermolecular contacts, and least-squares planes for complex **5** (16 pages). Ordering information is given on any current masthead page.

OM9307646

(27) See, for example: Alberty, R. A. *Physical Chemistry*; John Wiley and Sons: New York, 1983; Chapt. 17.
(28) Simpson, R. D.; Bergman, R. G. *Organometallics* **1992**, *11*, 4306.
(29) (a) Lindner, E.; Grimmer, R.; Weber, H. *Angew. Chem. Int. Ed. Engl.* **1970**, *9*, 639. (b) Lindner, E.; Grimmer, R. *J. Organomet. Chem.* **1970**, *25*, 493.
(30) See for example: Brunner, H.; Hammer, B.; Bernal, I.; Draux, M. *Organometallics* **1983**, 2, 1595 and ref cited therein.